

Honest calibration assessment for binary outcome predictions

Timo Dimitriadis^{1,2}, Lutz Dümbgen³, Alexander Henzi³, Marius Puke⁴, and Johanna Ziegel³

¹Heidelberg University, Germany

²Heidelberg Institute for Theoretical Studies (HITS), Germany

³University of Bern, Switzerland

⁴University of Hohenheim, Germany

timo.dimitriadis@awi.uni-heidelberg.de, lutz.duembgen@stat.unibe.ch,
alexander.henzi@stat.unibe.ch, marius.puke@uni-hohenheim.de,
johanna.ziegel@stat.unibe.ch

March 9, 2022

Abstract

Probability predictions from binary regressions or machine learning methods ought to be calibrated: If an event is predicted to occur with probability x , it should materialize with approximately that frequency, which means that the so-called calibration curve $p(x)$ should equal the bisector for all x in the unit interval. We propose honest calibration assessment based on novel confidence bands for the calibration curve, which are valid only subject to the natural assumption of isotonicity. Besides testing the classical goodness-of-fit null hypothesis of perfect calibration, our bands facilitate inverted goodness-of-fit tests whose rejection allows for the sought-after conclusion of a sufficiently well specified model. We show that our bands have a finite sample coverage guarantee, are narrower than existing approaches, and adapt to the local smoothness and variance of the calibration curve p . In an application to model predictions of an infant having a low birth weight, the bounds give informative insights on model calibration.

Keywords: Binary regression, calibration validation, isotonic regression, confidence band, goodness-of-fit, universally valid inference

1 Introduction

Let $x_1 \leq \dots \leq x_n$ be given covariates in $[0, 1]$ and $Y_1, \dots, Y_n \in \{0, 1\}$ independent binary observations such that $\mathbb{P}(Y_i = 1) = p(x_i)$ for some unknown function $p: [0, 1] \rightarrow [0, 1]$. In practice, the covariates can be probability predictions for the components of $\mathcal{Y} := (Y_i)_{i=1}^n$, e.g., stemming from a test sample of binary regressions, machine learning methods, or any other statistical model for binary data. A reliable interpretation of these predictions relies on the property of calibration, meaning that the so-called calibration curve p is sufficiently close to the identity. For instance, if a fetus is predicted to have a low birth weight with probability $x = 5\%$, decisions on a potential medical treatment rely on this probability prediction being accurate enough, $|p(x) - x| < \varepsilon$ for some small $\varepsilon > 0$.

Testing calibration, closely related to goodness-of-fit testing, is crucial in applications (Tutz, 2011; Hosmer et al., 2013) and is still regularly carried out by the classical test of Hosmer and Lemeshow (1980), which groups the predictions x_i into bins and applies a χ^2 -test. It is however subject to multiple criticisms: First, its ad hoc choice of bins can result in untenable

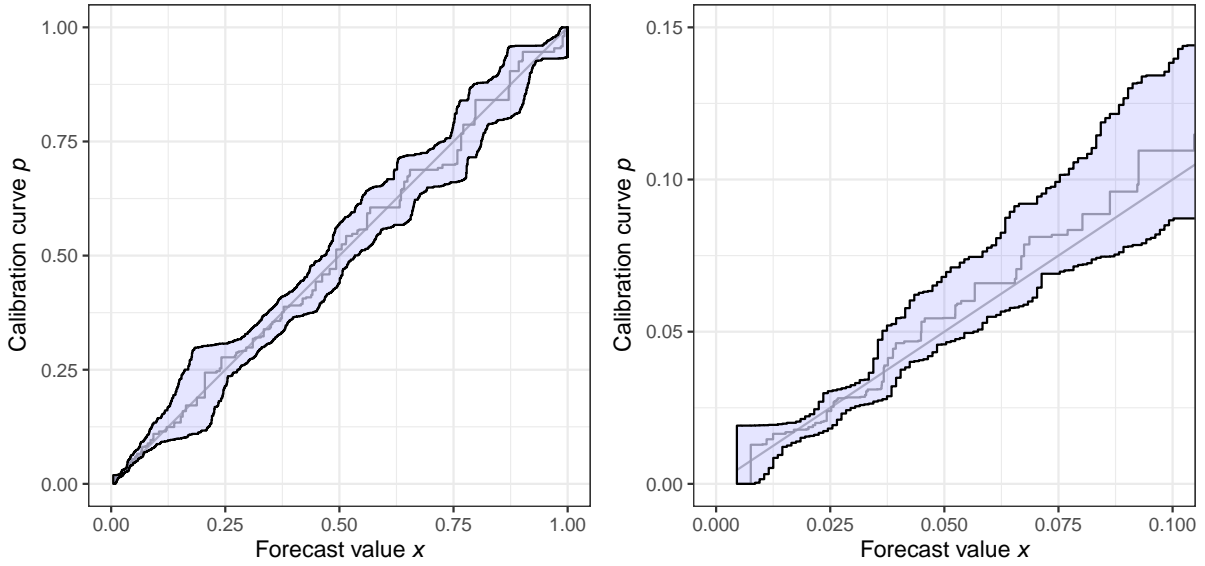


Figure 1: Left: Calibration bands for the first model specification of the low birth weight application in Section 6. The blue band denotes the calibration band and the grey step function the isotonic regression estimate. Right: Magnified version focusing on predicted probabilities below 10%.

instabilities (Bertolini et al., 2000; Allison, 2014). Second, placing the hypothesis of calibration in the null only allows for rejecting calibration rather than showing that a model is sufficiently well calibrated, where the latter would be highly desirable for applied researchers. Third, the test rejects essentially all, even acceptably well-specified models in large samples (Nattino et al., 2020a; Paul et al., 2013), resulting in calls for a goodness-of-fit tests with inverted hypotheses (Nattino et al., 2020b).

We propose a statistically sound solution to these criticisms by constructing honest, simultaneous confidence bands (L^α, U^α) for the function p . That is, for a given small number $\alpha \in (0, 1)$, we compute data-dependent functions $L^\alpha = L^\alpha(\cdot, \mathcal{Y})$ and $U^\alpha = U^\alpha(\cdot, \mathcal{Y})$ on $[0, 1]$ such that

$$\mathbb{P}\{L^\alpha \leq p \leq U^\alpha \text{ on } [0, 1]\} \geq 1 - \alpha, \quad (1)$$

which we call calibration band. It allows for the desirable conclusion that with confidence $1 - \alpha$, the true calibration curve p lies inside the band, simultaneously for all values of the predicted probabilities.

Hence, it resolves the above mentioned criticisms of classical goodness-of-fit tests. Figure 1 shows the bands in a large data example for probit model predictions for the binary outcome of a fetus having a low birth weight. See Section 6 for additional details. The test of Hosmer and Lemeshow clearly rejects calibration even though our bands indicate a well-calibrated model, especially for the, in this application, most important region of small probability predictions shown in the magnified right panel of the figure. Our bands also nest a goodness-of-fit test with classical hypotheses by checking whether the band contains the bisector $b(x) = x$ for all relevant values $x \in [0, 1]$. It is important to notice that even though we build our bands on the model predictions, the methodology applies equally to both, causal and predictive regressions. An open-source implementation in the statistical software R is available under <https://github.com/marius-cp/calibrationband>.

Our confidence bands are valid in finite samples subject only to the mild assumption that the function p is increasing,

$$p(x) \leq p(x'), \quad 0 \leq x \leq x' \leq 1, \quad (2)$$

which is natural in the context of assessing calibration as decreasing parts of the calibration curve p can be dismissed as nonsensical predictions resulting from severely misspecified models (Dimitriadis et al., 2021; Roelofs et al., 2020). As can be expected for a non-parametric, pathwise and almost universally valid confidence band, we require large data sets of at least above 5 000 observations to obtain sensibly narrow bands. These are exactly the sample sizes where the classical goodness-of-fit tests become uninformative by rejecting all models in applications. For example, in a simulation study on assessing a logistic regression model with minor misspecification, Kramer and Zimmerman (2007) find that the Hosmer-Lemeshow test at level $\alpha = 0.1$ achieves a power of 18.5% for $n = 5\,000$ and essentially 100% for $n = 50\,000$.

A theoretical analysis shows that the proposed confidence band adapts locally to the smoothness of the function p and to the variance of the observations. Adaptivity to the smoothness means that the width of the bands decreases faster with the sample size n in regions where p is constant, and at a slower rate where p is steeper. This property is known for more general confidence bands for a monotone mean function developed by Yang and Barber (2019), which are proved to be more conservative than our bands in the case of binary outcomes. Adaptivity to the variance means that the band is substantially narrower at x if $p(x)$ is close to zero or one, compared to $p(x)$ near 0.5. In many practical applications, including the low birth weight predictions analyzed in this article, predicted probabilities close to zero or one are of most relevance and a sharp assessment of calibration is particularly important.

Existing methods for the construction of confidence bands in this setting are rare with the following two exceptions: First, Nattino et al. (2014) propose the use of confidence bands based on a parametric assumption on the function p , which we show to have incorrect coverage in almost all of our simulation settings. Second, the nonparametric bands of Yang and Barber (2019) are valid but shown to be wider than our bands as we show in theory and simulations.

We explain the absence of competing methods by their theoretical difficulties. Using asymptotic theory of the isotonic regression estimator is complicated as it requires the estimation of nuisance quantities such as the derivative of the unknown function p , the convergence rate depends on the functional form of p , it is subject to more restrictive assumptions and only results in bands with a pointwise interpretation (Wright, 1981). Resampling schemes are theoretically found to be inconsistent for the isotonic regression (Sen et al., 2010; Guntuboyina and Sen, 2018). Other non-parametric approaches in the literature for constructing confidence bands for functions, many of them presented in the review by Hall and Horowitz (2013), are often pointwise, not simultaneous, and require the selection of tuning parameters that may lead to instabilities, similar to the choice of the bins in the Hosmer-Lemeshow test. In contrast, the confidence bands proposed here are simple to compute and do not involve any implementation decisions resulting in a stable and reproducible method as recently called for by Stodden et al. (2016); Yu and Kumbier (2020).

2 Construction of the confidence bands

In what follows we focus on confidence bounds $L_i^\alpha = L_i^\alpha(\mathcal{Y})$ and $U_i^\alpha = U_i^\alpha(\mathcal{Y})$ for $p_i = p(x_i)$, where $1 \leq i \leq n$. Indeed, if

$$\mathbb{P}(L_i^\alpha \leq p_i \leq U_i^\alpha \text{ for } 1 \leq i \leq n) \geq 1 - \alpha,$$

then

$$\begin{aligned} U^\alpha(x) &= U_i^\alpha, \quad x \in (x_{i-1}, x_i], \quad 1 \leq i \leq n+1, \\ L^\alpha(x) &= L_i^\alpha, \quad x \in [x_i, x_{i+1}), \quad 0 \leq i \leq n, \end{aligned}$$

defines a confidence band (L^α, U^α) satisfying (1) with the auxiliary values $x_0 := -\infty$, $L_0^\alpha := 0$ and $x_{n+1} := \infty$, $U_{n+1}^\alpha := 1$.

Our confidence bands are based on the classical confidence bounds of [Clopper and Pearson \(1934\)](#) for a binomial parameter. Suppose that Z is a binomial random variable with parameters m and $q \in [0, 1]$. For $\delta \in (0, 1)$ let

$$\begin{aligned} u^\delta(Z, m) &= \max\{\xi \in [0, 1] : \text{pbin}(Z, m, \xi) \geq \delta\} \\ &= \begin{cases} \text{qbeta}(1 - \delta, Z + 1, m - Z), & Z < m, \\ 1, & Z = m, \end{cases} \\ \ell^\delta(Z, m) &= \min\{\xi \in [0, 1] : \text{pbin}(Z - 1, m, \xi) \leq 1 - \delta\} \\ &= \begin{cases} \text{qbeta}(\delta, Z, m + 1 - Z), & Z > 0, \\ 0, & Z = 0. \end{cases} \end{aligned}$$

Here $\text{pbin}(\cdot, m, \xi)$ denotes the distribution function of the binomial distribution with parameters m and ξ , while $\text{qbeta}(\cdot, a, b)$ stands for the quantile function of the beta distribution with parameters $a, b > 0$. Then

$$\mathbb{P}\{q \leq u^\delta(Z, m)\} \geq 1 - \delta \quad \text{and} \quad \mathbb{P}\{q \geq \ell^\delta(Z, m)\} \geq 1 - \delta.$$

For the representation of $\ell^\delta(Z, m)$ and $u^\delta(Z, m)$ in terms of beta quantiles we refer to [Johnson et al. \(2005\)](#).

Assumption (2) allows to construct confidence bands for p as follows. For arbitrary indices $1 \leq j \leq k \leq n$, the random sum

$$Z_{jk} = \sum_{i=j}^k Y_i$$

is stochastically larger than a binomial random variable with parameters $n_{jk} = k - j + 1$ and p_j , and it is stochastically smaller than a binomial variable with parameters n_{jk} and p_k . Thus, as explained in Lemma B.1,

$$\mathbb{P}\{p_j \leq u^\delta(Z_{jk}, n_{jk})\} \geq 1 - \delta, \quad \mathbb{P}\{p_k \geq \ell^\delta(Z_{jk}, n_{jk})\} \geq 1 - \delta. \quad (3)$$

If we combine these bounds for all pairs (j, k) in a given set \mathcal{J} , then we may claim with confidence $1 - 2|\mathcal{J}|\delta$ that simultaneously for all $(j, k) \in \mathcal{J}$,

$$p_i \leq u^\delta(Z_{jk}, n_{jk}) \quad \forall i \leq j, \quad p_i \geq \ell^\delta(Z_{jk}, n_{jk}) \quad \forall i \geq k.$$

Specifically, let \mathcal{J} be the set of all index pairs (j, k) such that $j \leq k$ and $x_{j-1} < x_j$ and $x_k < x_{k+1}$. If there are tied covariate values, \mathcal{J} selects the outermost indices of the tied values. Hence, if $\{x_1, \dots, x_n\}$ contains $N \leq n$ different points, then $|\mathcal{J}| = (N^2 + N)/2$. Consequently, for a given confidence level $1 - \alpha \in (0, 1)$, we may combine the bounds $u^\delta(Z_{jk}, n_{jk})$ and $\ell^\delta(Z_{jk}, n_{jk})$ with $\delta = \alpha/(N^2 + N)$ to obtain a first confidence band.

Theorem 2.1. *For $1 \leq i \leq n$ let*

$$U_i^{\alpha, \text{raw}} = \min_{(j, k) \in \mathcal{J}: x_j \geq x_i} u^{\alpha/(N^2 + N)}(Z_{jk}, n_{jk}), \quad (4)$$

$$L_i^{\alpha, \text{raw}} = \max_{(j, k) \in \mathcal{J}: x_k \leq x_i} \ell^{\alpha/(N^2 + N)}(Z_{jk}, n_{jk}). \quad (5)$$

If p satisfies the isotonicity assumption (2), then the resulting confidence band $(L_i^{\alpha, \text{raw}}, U_i^{\alpha, \text{raw}})$ satisfies requirement (1).

In the definition (4), taking the minimum over index pairs (j, k) with $x_j \geq x_i$ is equivalent to the minimum over $j \geq i$ if $x_1 < \dots < x_n$. When there are ties in the covariate, it is possible

that the minimum is attained with an index $j < i$ but $x_j = x_i$. Analogously, it is possible that the maximum in (5) is attained with an index $k > i$ but $x_k = x_i$.

The confidence band proposed in Theorem 2.1 has two potential drawbacks. First, a natural nonparametric estimator for the function p under the assumption (2) is given by a minimizer \hat{p} of $\sum_{i=1}^n \{h(x_i) - Y_i\}^2$ over all isotonic functions $h: [0, 1] \rightarrow [0, 1]$ (Dimitriadis et al., 2021). This minimizer is unique on the set $\{x_1, \dots, x_n\}$. But there is no guarantee that $L^{\alpha, \text{raw}} \leq \hat{p} \leq U^{\alpha, \text{raw}}$. Second, the upper and lower bounds in (4) and (5) may even cross, resulting in an empty, and hence, nonsensical confidence band. These problems can be dealt with by using the non-crossing confidence band $(L^{\alpha, \text{nc}}, U^{\alpha, \text{nc}})$ with

$$L_i^{\alpha, \text{nc}} = \min\{L_i^{\alpha, \text{raw}}, \hat{p}(x_i)\}, \quad U_i^{\alpha, \text{nc}} = \max\{L_i^{\alpha, \text{raw}}, \hat{p}(x_i)\}. \quad (6)$$

This band satisfies $L^{\alpha, \text{nc}} \leq \hat{p} \leq U^{\alpha, \text{nc}}$ on $[0, 1]$, no matter how $\hat{p}(x)$ is defined for $x \notin \{x_1, \dots, x_n\}$. Our simulations experiments indicate that $(L^{\alpha, \text{raw}}, U^{\alpha, \text{raw}}) = (L^{\alpha, \text{nc}}, U^{\alpha, \text{nc}})$ with probability $\gg 1 - \alpha$; see Section 5 for details.

A potential obstacle in the practical application of the confidence bands proposed in this section is that their computation requires $\mathcal{O}(N^2)$ steps. This can be relieved by reducing the number of distinct values in the covariate by rounding, which often has almost no visible effect on the appearance of the bands. If differences in the covariate smaller than K^{-1} for some $K \in \mathbb{N}$ are regarded as negligible, one can round up x_1, \dots, x_n to the next multiple of K^{-1} for the computation of the upper bound, and round off x_1, \dots, x_n to the next lower multiple of K^{-1} to compute the lower bound. This still yields a valid confidence band for the function p but guarantees that $N \leq K + 1$, which also implies a less conservative correction of the confidence level. The number $K \in \mathbb{N}$ should not be too small since the resulting confidence bands are constant on intervals of length K^{-1} thereby limiting their adaptivity.

3 Relation to Yang and Barber (2019)

The methods of Yang and Barber (2019) may be adapted to the present regression setting with covariates $x_1 \leq \dots \leq x_n$ as follows: With the isotonic estimator \hat{p} introduced before, let

$$Z_{jk}^{\text{iso}} = \sum_{i=j}^k \hat{p}(x_i).$$

Set

$$U_i^{\alpha, \text{YB}} = \min_{(j,k) \in \mathcal{J}: x_j \geq x_i} \left[\frac{Z_{jk}^{\text{iso}}}{n_{jk}} + \sqrt{\frac{\log\{(N^2 + N)/\alpha\}}{2n_{jk}}} \right], \quad (7)$$

$$L_i^{\alpha, \text{YB}} = \max_{(j,k) \in \mathcal{J}: x_k \leq x_i} \left[\frac{Z_{jk}^{\text{iso}}}{n_{jk}} - \sqrt{\frac{\log\{(N^2 + N)/\alpha\}}{2n_{jk}}} \right]. \quad (8)$$

This defines a confidence band $(L^{\alpha, \text{YB}}, U^{\alpha, \text{YB}})$ with the following property:

$$\mathbb{P}\{L^{\alpha, \text{YB}} \leq \tilde{p} \leq U^{\alpha, \text{YB}} \text{ on } [0, 1]\} \geq 1 - \alpha, \quad (9)$$

where $\tilde{p}: [0, 1] \rightarrow [0, 1]$ is any fixed isotonic function minimizing $\sum_{i=1}^n \{\tilde{p}(x_i) - p_i\}^2$. Thus one obtains a confidence band with guaranteed coverage probability $1 - \alpha$ for an isotonic approximation of p , even if (2) is violated. The proof of (9) follows from the arguments of Yang and Barber (2019), noting that the random variables Y_i are subgaussian with scale parameter $\sigma = 1/2$. That means, $\mathbb{E} \exp(t(Y_i - p_i)) \leq \exp(\sigma^2 t^2/2)$ for all $t \in \mathbb{R}$, which implies that for arbitrary $\eta \geq 0$,

$$\mathbb{P}\{\pm(Z_{jk} - \mathbb{E} Z_{jk}) \geq \eta\} \leq \exp(-2n_{jk}\eta^2),$$

see [Hoeffding \(1963\)](#). The following result shows that the confidence bands $(L^{\alpha,\text{raw}}, U^{\alpha,\text{raw}})$ and $(L^{\alpha,\text{nc}}, U^{\alpha,\text{nc}})$ are always contained in the band $(L^{\alpha,\text{YB}}, U^{\alpha,\text{YB}})$.

Theorem 3.1. *For all $\alpha \in (0, 1)$ and any data vector $\mathcal{Y} \in \{0, 1\}^n$,*

$$L^{\alpha,\text{YB}} \leq L^{\alpha,\text{nc}} \leq L^{\alpha,\text{raw}}, \quad U^{\alpha,\text{raw}} \leq U^{\alpha,\text{nc}} \leq U^{\alpha,\text{YB}} \quad \text{on } [0, 1].$$

For the applications considered in the present paper, the validity of a confidence band in case of p violating (2) is not essential. It should be mentioned, however, that the band $(L^{\alpha,\text{YB}}, U^{\alpha,\text{YB}})$ has a computational advantage. For the computation of $U_i^{\alpha,\text{YB}}$ in (7), it suffices to take the minimum over endpoints of constancy regions of \hat{p} , that is, all $(j, k) \in \mathcal{J}$ such that $j = \min(s: x_s \geq x_i)$ and $\hat{p}(x_k) < \hat{p}(x_{k+1})$ or $k = n$, see [Proposition B.3](#) in the appendix. Likewise, for the computation of $L_i^{\alpha,\text{YB}}$ in (8), it suffices to take the maximum over all $(j, k) \in \mathcal{J}$ such that $\hat{p}(x_{j-1}) < \hat{p}(x_j)$ or $j = 1$ and $k = \max(s: x_s \leq x_i)$. While the computation of $(L^{\alpha,\text{raw}}, U^{\alpha,\text{raw}})$ or $(L^{\alpha,\text{nc}}, U^{\alpha,\text{nc}})$ requires $\mathcal{O}(N^2)$ steps, the following lemma implies that the computation of $(L^{\alpha,\text{YB}}, U^{\alpha,\text{YB}})$ requires only $\mathcal{O}(N \min\{n^{2/3}, N\})$ steps.

Lemma 3.2. *The cardinality of $\{\hat{p}(x_i): 1 \leq i \leq n\}$ is smaller than $3n^{2/3}$.*

4 Theoretical properties of the confidence bands

This section illustrates consistency and adaptivity properties of the confidence band $(L_n^{\alpha,\text{raw}}, U_n^{\alpha,\text{raw}})$, where the subscript n indicates the sample size, and we consider a triangular scheme of observations $(x_i, Y_i) = (x_{ni}, Y_{ni})$, $1 \leq i \leq n$. We are interested in situations in which the observed covariates x_{ni} could be the realizations of the order statistics of a random sample. Thus we have to extend the framework of [Yang and Barber \(2019\)](#) and consider the following assumption.

(A) Let $\text{Leb}(\cdot)$ denote Lebesgue measure, and let $W_n(B) = \sum_{i=1}^n \mathbf{1}(x_{ni} \in B)$ for $B \subset [0, 1]$. There exist constants $C_1, C_2 > 0$ such that for sufficiently large n ,

$$W_n(B) \geq C_1 n \text{Leb}(B)$$

for arbitrary intervals $B \subset [0, 1]$ such that $\text{Leb}(B) \geq C_2 \log(n)/n$.

This assumption comprises the setting of [Yang and Barber \(2019\)](#). Let G be a differentiable distribution function on $[0, 1]$ such that G' is bounded away from 0. If $x_{ni} = G^{-1}(i/n)$ for $1 \leq i \leq n$, then (A) is satisfied for any $C_1 < \inf_{[0,1]} G'$ and arbitrary $C_2 > 0$. The arguments in [Mösching and Dümbgen \(2020, Section 4.3\)](#) can be modified to show that if x_{n1}, \dots, x_{nn} are the order statistics of n independent random variables with distribution function G , then Condition (A) is satisfied almost surely, provided that $C_1, C_2 > 0$ are chosen appropriately.

Theorem 4.1. *Suppose that condition (A) is satisfied. Let $\rho_n = \log(n)/n$.*

(i) *Suppose that p is constant on some non-degenerate interval $[a, b] \subset [0, 1]$. Then*

$$\sup_{x \in [a, b']} \{U_n^{\alpha,\text{raw}}(x) - p(x)\}^+ + \sup_{x \in [a', b]} \{p(x) - L_n^{\alpha,\text{raw}}(x)\}^+ = \mathcal{O}_p(\rho_n^{1/2})$$

for any fixed interval $[a', b'] \subset (a, b)$.

(ii) *Suppose that p is Lipschitz-continuous on a non-degenerate interval $[a, b] \subset [0, 1]$. Then*

$$\sup_{x \in [a, b - \rho_n^{1/3}]} \{U_n^{\alpha,\text{raw}}(x) - p(x)\}^+ + \sup_{x \in [a + \rho_n^{1/3}, b]} \{p(x) - L_n^{\alpha,\text{raw}}(x)\}^+ = \mathcal{O}_p(\rho_n^{1/3}).$$

(iii) *Suppose that for some constant $\gamma \geq 1$, $p(x) = \mathcal{O}(x^\gamma)$ as $x \rightarrow 0$. Then,*

$$\sup_{x \in [0, 1]} \frac{\mathbb{E}\{U_n^{\alpha,\text{raw}}(x)\}}{x^\gamma + \rho_n^{1/2}} = \mathcal{O}(1).$$

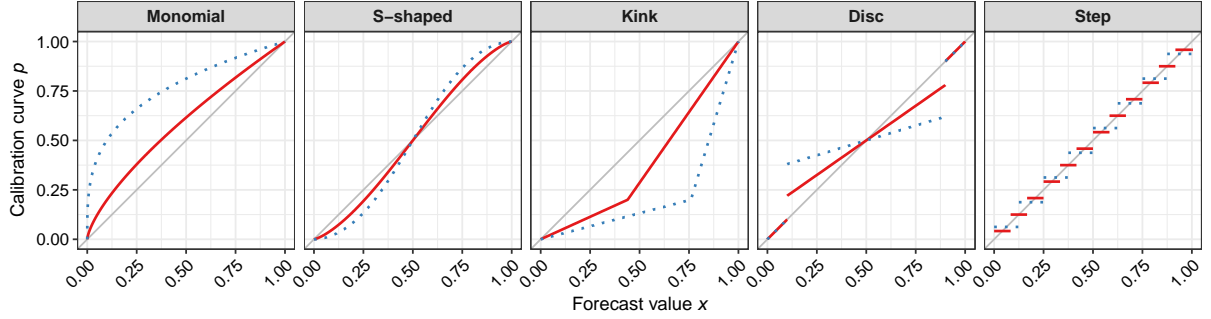


Figure 2: Illustration of the five simulated calibration curves $p_s(\cdot)$, where the solid red line corresponds to the shape parameter value $s = 0.3$ and the dashed blue line to $s = 0.7$.

An analogous statement holds for the lower bound $L_n^{\alpha, \text{raw}}$.

(iv) Suppose that p is discontinuous at some point $x_o \in (0, 1)$. Then for any number q strictly between $p(x_o-)$ and $p(x_o+)$ and a suitable constant $C > 0$,

$$U_n^{\alpha, \text{raw}}(x_o - C\rho_n) < q < L_n^{\alpha, \text{raw}}(x_o + C\rho_n)$$

with asymptotic probability one as $n \rightarrow \infty$.

Parts (i-ii) of this theorem are analogous to the results of [Yang and Barber \(2019, Sections 4.4 and 4.6\)](#). Part (iii) demonstrates that our bounds are particularly accurate in regions where $p(x)$ is close to 0 or 1. Presumably, the conclusions in parts (iii-iv) are not satisfied for the confidence band $(L_n^{\alpha, \text{YB}}, U_n^{\alpha, \text{YB}})$.

5 Simulations

Here, we illustrate that our calibration bands have correct coverage in the sense of (1) and are narrower than existing techniques. We consider both, the raw method in (4) and (5) and the non-crossing variant in (6). Both methods are combined with the rounding technique to three digits after the comma as described in the end of Section 2 in order to facilitate faster computation at a minimal cost in accuracy. For comparison, we use the isotonic bands of [Yang and Barber \(2019\)](#) given in (7) and (8) with a minimal variance factor of $\sigma^2 = 1/4$ and the parametric bands of [Nattino et al. \(2014\)](#), implemented in the `GivitiR` package in the statistical software R ([R Core Team, 2022](#)). Replication material for the simulations and applications is available under https://github.com/marius-cp/replication_DDHPZ22.

We use 1000 replications, a significance level of $\alpha = 0.05$ and simulate the predictions $X \sim U[0, 1]$. The binary outcomes are generated by $Y \sim \text{Bern}\{p_s(X)\}$ based on five distinct functional forms of the calibration curve $p_s(x)$ for $x \in [0, 1]$ depending on a shape parameter $s \in \mathcal{S} := \{0, 0.1, \dots, 1\}$. All specifications of $p_s(x)$ satisfy the isotonicity assumption in (2) and they cover smooth, non-smooth as well as discontinuous setups. The choice $s = 0$ results in perfectly calibrated forecasts with $p_0(x) = x$ whereas the misscalibration increases with s . In particular, we consider the following specifications, which are illustrated in Figure 2 for two exemplary shape values $s \in \{0.3, 0.7\}$.

1. Monomial: First, we use a calibration curve defined by $p_s(x) = x^{1-s}$, where $s \in \mathcal{S} \setminus \{1\}$. This is already used in the simulations assessing the CORP reliability diagram in [Dimitriadis et al. \(2021, Appendix A\)](#).
2. S-shaped: Second, the calibration curve follows an S-shaped form $p_s(x) = (1 + ((1-x)/x)^{1+s})^{-1}$, where $s \in \mathcal{S}$ pronounces the curves for larger values of s .

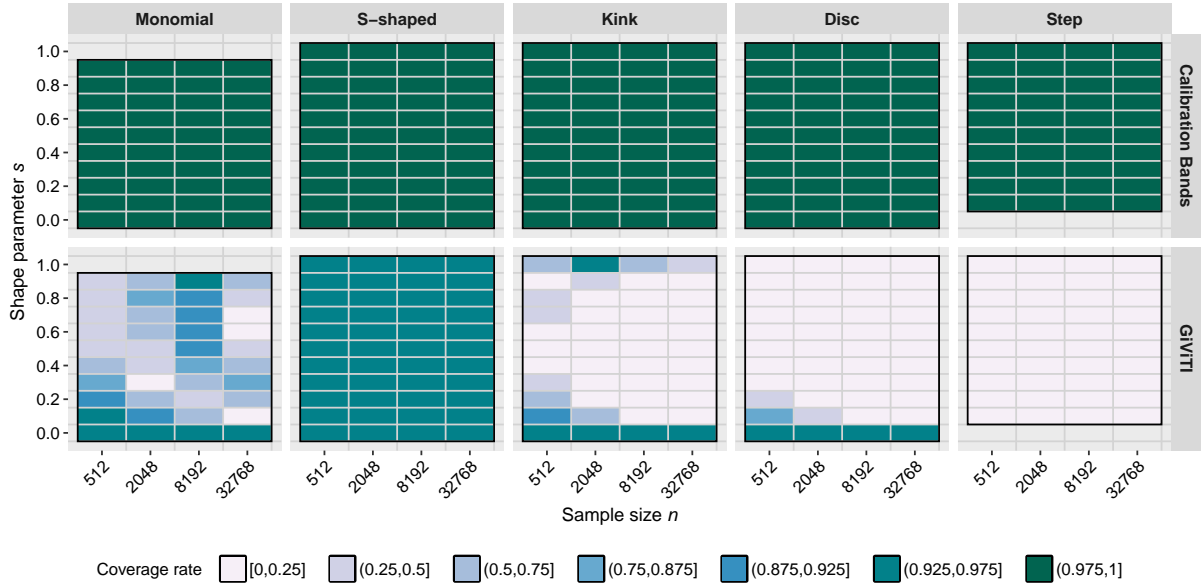


Figure 3: Empirical coverage rates of our calibration bands and the GiVITI bands for $1 - \alpha = 0.95$ averaged over all forecast values $x \in [0, 1]$, for the five specifications of the calibration curve $p_s(\cdot)$, different shape values s and a range of sample sizes n . Notice that the choices $s = 1$ in the monomial, and $s = 0$ in step specification are not defined.

3. Kink: Third, $p_s(x)$ linearly interpolates the points $(0, 0)$, $(0.2 + 0.8s, 0.2)$ and $(1, 1)$ for $s \in \mathcal{S}$, resulting in a kink at the point $(0.2 + 0.8s, 0.2)$ for all $s > 0$.
4. Disc: Fourth, we have a perfect calibration $p_s(x) = x$ close to the borders $x \notin (0.1, 0.9)$, and a rotating, miscalibrated disc, $p_s(x) = (1 - s)x + s/2$ within $x \in [0.1, 0.9]$, where the rotation increases with $s \in \mathcal{S}$.
5. Step: Fifth, we use a step function with $s^* \in \{5, 6, \dots, 14\}$ equidistant steps in the unit interval. Formally, it is given by $p_s(x) = \{ \lfloor s^*x \rfloor + \mathbf{1}(x \neq 1) \} / s^*$, where $s^* = 15 - 10s$ and $s \in \mathcal{S} \setminus \{0\}$. Notice that this choice does not nest a correctly specified model, but its misspecification still increases with s .

Figure 3 presents the average coverage rates for a range of sample sizes between 512 and 32768. We find that, as predicted by our theory, our calibration bands have conservative coverage throughout all simulation setups and sample sizes. We observe coverage rates between 0.998 and 1, with the majority of 179 out of the 212 displayed coverage values being exactly one. We dispense with a presentation of the coverage rates of the non-crossing and [Yang and Barber \(2019\)](#) bands, as both are guaranteed to be larger by Theorem 3.1. The non-crossing bands differ from the raw ones in less than one out of a hundred thousand simulated forecast values. These deviations occur exclusively for large values of s in the Step and Disc specifications within constancy regions of the calibration curve p .

The parametric bands of [Nattino et al. \(2014\)](#) rarely achieve correct coverage rates unless in the cases $s = 0$ and for the S-shaped calibration curve. This can be explained as these bands are based on the assumption of a certain parametric form of $p_s(x)$, which is rarely satisfied. The results get worse for the non-smooth and the two discontinuous specifications.

Figure 4 displays the average widths of the non-crossing and [Yang and Barber \(2019\)](#) bands. We present the theoretically wider non-crossing bands instead of the raw versions thereof. Their average widths is however non-distinguishable in these displays. We fix a medium degree of miscalibration $s = 0.5$. The upper plot panel displays the widths averaged over all simulation runs and forecast values depending on the sample size n . We find that the size of both bands

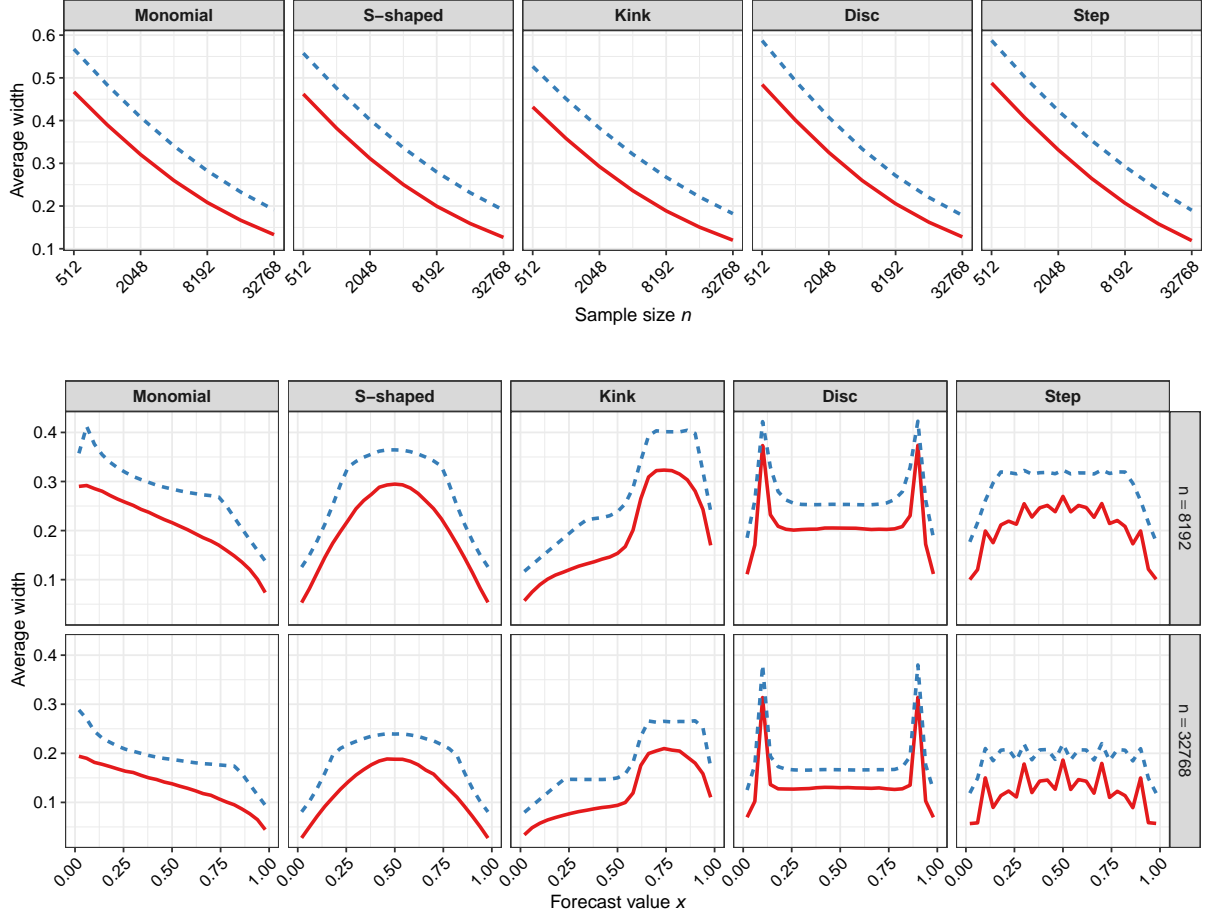


Figure 4: Top: Average empirical widths of the 95% confidence bands by sample size for the non-crossing and [Yang and Barber \(2019\)](#) bands for each of the five specifications of $p_s(x)$ given in the main text for a fixed degree of misspecification $s = 0.5$. Bottom: Average empirical widths by forecast value x for two sample sizes. In both panels, the solid red line corresponds to the non-crossing bands and the dashed blue line to the [Yang and Barber \(2019\)](#) bands.

shrinks with n and that we can reconfirm the ordering established in Theorem 3.1. We further see that our bands are only narrow enough for practical use in large samples. The relative gain in width of our bands is the highest for large sample sizes, exactly for which we propose the application of our method for calibration validation. It is worth noting that the bands of [Yang and Barber \(2019\)](#) are more generally valid than for the special case of binary observations.

The lower plot panel shows the widths averaged over the simulation replications, but depending on the forecast value x for two selected sample sizes. It shows that the relative gains in width upon the bands of [Yang and Barber \(2019\)](#) are particularly pronounced close to the edges of the unit interval. These regions of predicted probabilities close to zero or one are often of the highest interest in assessing calibration as for example in the subsequent application to low birth weight probability predictions.

6 Application: Predicting low birth weight probabilities

We apply our calibration bands to binary regressions predicting the probability of a fetus having a low birth weight, defined as weighing less than 2500 grams at birth ([World Health Organization, 2015](#)). We use U.S. Natality Data from the [National Center for Health Statistics \(2017\)](#), which provides demographic and health data for 3 864 754 births in the year 2017. For the data set at

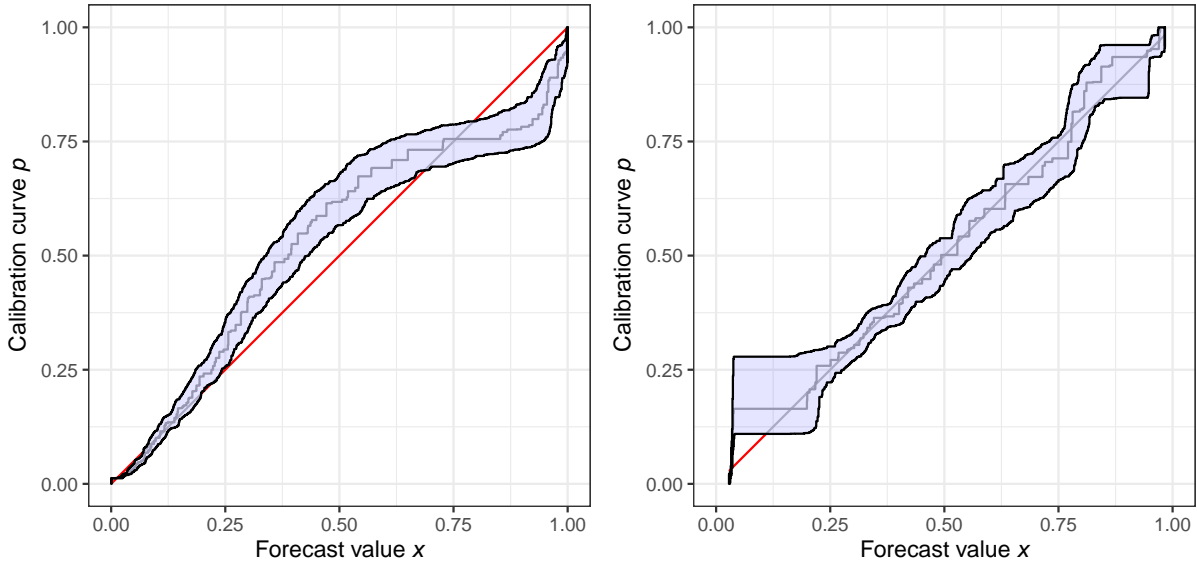


Figure 5: Calibration bands for the second model specification on the left and for the third specification on the right for the low birth weight application. The blue band denotes the calibration band and the grey step function the isotonic regression estimate. The bisector is given in red color whenever it is not contained in the calibration band.

hand, a low birth weight is observed in 8.1% of the cases.

We estimate three binary regression models by maximum likelihood on the same randomly drawn subset that contains all but 1 000 000 observations that we leave for external model validation. All three models contain standard risk factors such as the mother's age, body mass index and smoking behavior but they differ as follows. The first model uses a probit link function, and the explanatory variable week of gestation is categorized into four left-closed and right-open intervals with lower interval limits of 0, 28, 32 and 37 weeks, pertaining to the standard definitions of the World Health Organization of extremely, very, moderate and non preterm (Quinn et al., 2016). Through this categorization, the model specification can capture the week of gestation in a non-linear fashion. In contrast, the second model uses the week of gestation as a continuous explanatory variable and the third specification employs the cauchit instead of the probit link function, which is known to produce less confident predictions close to zero and one (Koenker and Yoon, 2009). Additional details of the model specifications are given in Appendix 1.

The classical Hosmer-Lemeshow test rejects perfect calibration of all three models with p-values of essentially zero for both, internal and external model validation, which leaves an applied researcher without any useful conclusions on model calibration. We show our calibration bands for the first model in Figure 1 and for the other two model specifications in Figure 5. We use the non-crossing method with rounding to three digits with a confidence level of $1 - \alpha = 95\%$.

For the first model, the calibration bands encompass the bisector for all forecast values, meaning that we cannot reject the null hypothesis of perfect calibration at the 5% level. More importantly, we are 95% certain that the true calibration curve lies within the the band at any point $x \in [0, 1]$, implying that we are confident that the model is at least as well calibrated as specified by the band. This is especially notable in the important region of predictions below 10% in the magnified right panel of Figure 1, where the confidence bands are remarkably close to the bisector implying a particularly well calibrated model. E.g., we are confident to conclude that a prediction of $x = 5\%$ occurs on average with a probability between 4.6% and 6.7%.

In contrast, we reject calibration for both, the second and third model specifications as shown in Figure 5. However, these bands are much more informative than a simple test rejection as they

directly show the exact form of model miscalibration. E.g., for the second model specification, we can conclude that the predicted probabilities are particularly miscalibrated for values larger than 20% whereas the third specification entails miscalibrated probabilities for predictions below 10% that are presumably of the highest importance for medical decision making. While small predicted values from the second specification might still be treated as relatively reliable, they should be interpreted with great caution when stemming from the third model. The wider bands for the third model specification between predicted probabilities of 5% and 20% are caused by relatively little predictions in this interval.

Acknowledgement

A. Henzi and J. Ziegel gratefully acknowledge financial support from the Swiss National Science Foundation.

A Model specifications in the low birth weight application

We give some additional details on the model specifications of the application here. The first two models are based on the probit link function whereas the third one uses the cauchit link function (Koenker and Yoon, 2009). The second model uses the week of gestation as a continuous variable whereas the first and third models use the week of gestation as a categorical variable with left-closed and right-open intervals with lower interval limits of 0, 28, 32 and 37 weeks, which corresponds to the standard categorization of the World Health Organization (Quinn et al., 2016).

Additionally, all three models contain the following common explanatory variables: the mother's age and its squared term, her body mass index prior to pregnancy, her smoking behavior as a categorical variable with left-closed and right-open intervals with lower limits of 0, 1, 9, and 20 cigarettes per day averaged over all three trimesters, individual binary variables for mother's diabetes, any form of hypertension, mother's education below or equal to eight years, employed infertility treatments, a cesarean in a previous pregnancy, a preterm birth in a previous pregnancy, current multiple pregnancy, the sex of the unborn child, and an infection of one of the following: gonorrhea, syphilis, chlamydia, hepatitis b, hepatitis c. Additional details on the data are given in the user guide under <https://data.nber.org/nativity/2017/natl2017.pdf>.

B Proofs and Technical Lemmas

Lemma B.1. *Let Y_1, \dots, Y_m be independent Bernoulli variables with expectations $p_1 \leq \dots \leq p_m$, and let $Z = Y_1 + \dots + Y_m$. Then for any $\delta \in (0, 1)$,*

$$\mathbb{P}\{p_1 \leq u^\delta(Z, m)\} \geq 1 - \delta \quad \text{and} \quad \mathbb{P}\{p_m \geq \ell^\delta(Z, m)\} \geq 1 - \delta.$$

Proof of Lemma B.1. For the upper bound, note that $u^\delta(z, m)$ is increasing in z . If $b = \min\{z \in \{0, \dots, m\} : u^\delta(z, m) \geq p_1\}$, then $\mathbb{P}\{p_1 \leq u^\delta(Z, m)\} = \mathbb{P}(Z \geq b)$. By Shaked and Shanthikumar (2007, Example 1.A.25), Z is stochastically larger than \tilde{Z} with binomial distribution with parameters m and p_1 , so $\mathbb{P}(Z \geq b) \geq \mathbb{P}(\tilde{Z} \geq b) \geq 1 - \delta$, where the last inequality follows from the validity of the Clopper-Pearson confidence bounds. The proof for the lower bound is similar. \square

The proof of Theorem 3.1 uses standard results for isotonic least squares regression and the following inequalities of Hoeffding (1963, Theorem 1).

Lemma B.2. Let Y_1, Y_2, \dots, Y_m be independent random variables with values in $[0, 1]$ and expectations p_1, p_2, \dots, p_m . Suppose that $q = m^{-1} \sum_{i=1}^m p_i \in (0, 1)$, and set $\hat{q} = m^{-1} \sum_{i=1}^m Y_i$. Then for arbitrary $r \in [0, 1]$,

$$\begin{aligned}\mathbb{P}(\hat{q} \leq r) &\leq \exp\{-mK(r, q)\} \leq \exp\{-2m(r - q)^2\} \quad \text{if } r \leq q, \\ \mathbb{P}(\hat{q} \geq r) &\leq \exp\{-mK(r, q)\} \leq \exp\{-2m(r - q)^2\} \quad \text{if } r \geq q,\end{aligned}$$

where $K(r, q) := r \log(r/q) + (1 - r) \log[(1 - r)/(1 - q)]$.

Corollary 1. For integers $m \geq 1$, $z \in \{0, 1, \dots, m\}$ and any number $\delta \in (0, 1)$,

$$\begin{aligned}u^\delta(z, m) &\leq \max\{\xi \in [\hat{q}, 1] : K(\hat{q}, \xi) \leq \log(1/\delta)/m\} \leq \hat{q} + \sqrt{\log(1/\delta)/(2m)}, \\ \ell^\delta(z, m) &\geq \min\{\xi \in [0, \hat{q}] : K(\hat{q}, \xi) \leq \log(1/\delta)/m\} \geq \hat{q} - \sqrt{\log(1/\delta)/(2m)},\end{aligned}$$

where $\hat{q} = z/m$.

In addition, the proof of Theorem 3.1 makes use of the following proposition which is of independent interest, since it implies a more efficient method for computing the bounds of Yang and Barber (2019).

Proposition B.3. For an arbitrary observation vector $\mathcal{Y} \in \mathbb{R}^n$, let $\hat{p} : [0, 1] \rightarrow \mathbb{R}$ be an increasing function minimizing $\sum_{i=1}^n \{Y_i - \hat{p}(x_i)\}^2$. For some $\tau > 0$ and any index $1 \leq i \leq n$, let

$$U_i = \min_{(j, k) \in \mathcal{J}: x_j \geq x_i} \left(\frac{Z_{jk}^{\text{iso}}}{n_{jk}} + \frac{\tau}{\sqrt{n_{jk}}} \right), \quad L_i = \max_{(j, k) \in \mathcal{J}: x_k \leq x_i} \left(\frac{Z_{jk}^{\text{iso}}}{n_{jk}} - \frac{\tau}{\sqrt{n_{jk}}} \right).$$

Then, the minimum for U_i is attained at some $(j, k) \in \mathcal{J}$ such that $j = \min(s: x_s \geq x_i)$ and $\hat{p}(x_k) < \hat{p}(x_{k+1})$ or $k = n$. The maximum for L_i is attained at some $(j, k) \in \mathcal{J}$ such that $\hat{p}(x_{j-1}) < \hat{p}(x_j)$ or $j = 1$ and $k = \max(s: x_s \leq x_i)$.

Proof of Proposition B.3. Consider the statement about U_i . The claim about j follows from the fact that for fixed k , $Z_{jk}^{\text{iso}}/n_{jk}$ is increasing and $n_{jk} = n - j + k$ is decreasing in $j \leq k$. As to the upper index k , note that U_i is the minimum of $u_{jk} = Z_{jk}^{\text{iso}} n_{jk}^{-1} + \tau n_{jk}^{-1/2}$ over all $k \geq j = \min(s: x_s \geq x_i)$ such that $(j, k) \in \mathcal{J}$. Let $j \leq k_1 < k_2$ be indices such that $\hat{p}(x_k) = \hat{q}$ for $k_1 < k \leq k_2$. Then, for $k_1 \leq k \leq k_2$,

$$Z_{jk}^{\text{iso}} = Z_{jk_1}^{\text{iso}} + (k - k_1)\hat{q} = B + n_{jk}\hat{q}$$

with

$$B = Z_{jk_1}^{\text{iso}} - n_{jk_1}\hat{q} \begin{cases} \leq 0, \\ = 0 & \text{if } \hat{p}(x_j) = \hat{q}. \end{cases}$$

Consequently, for $k_1 \leq k \leq k_2$,

$$u_{jk} = \hat{q} + B n_{jk}^{-1} + \tau n_{jk}^{-1/2}$$

is a concave function of $n_{jk}^{-1} \in [n_{jk_2}^{-1}, n_{jk_1}^{-1}]$, and it is increasing in n_{jk}^{-1} if $\hat{q} = \hat{p}(x_j)$. This implies that

$$u_{jk} \geq \begin{cases} \min(u_{jk_1}, u_{jk_2}), \\ u_{jk_2} & \text{if } \hat{q} = \hat{p}(x_j). \end{cases}$$

Consequently, the minimum of u_{jk} over all $k \geq j$ is attained at some $k \geq j$ such that $\hat{p}(x_k) < \hat{p}(x_{k+1})$ or $k = n$, and this entails that $(j, k) \in \mathcal{J}$. The statement about L_i follows from the one about U_i when x_1, \dots, x_n are replaced by $1 - x_n, \dots, 1 - x_1$ and Y_1, \dots, Y_n by $-Y_n, \dots, -Y_1$. \square

Proof of Theorem 3.1. The inequalities $L_i^{\alpha, \text{nc}} \leq L_i^{\alpha, \text{raw}}$ and $U_i^{\alpha, \text{raw}} \leq U_i^{\alpha, \text{nc}}$, as well as $L_i^{\alpha, \text{YB}} \leq \hat{p}(x_i) \leq U_i^{\alpha, \text{YB}}$ hold by construction. It is therefore sufficient to show that $L_i^{\alpha, \text{YB}} \leq L_i^{\alpha, \text{raw}}$ and $U_i^{\alpha, \text{raw}} \leq U_i^{\alpha, \text{YB}}$. As to the inequality $U_i^{\alpha, \text{raw}} \leq U_i^{\alpha, \text{YB}}$, we know that $U_i^{\alpha, \text{YB}}$ equals

$$u_{jk}^{\text{YB}} = Z_{jk}^{\text{iso}} n_{jk}^{-1} + \tau n_{jk}^{-1/2}$$

for some $(j, k) \in \mathcal{J}$ with $j = \min\{s : x_s \geq x_i\}$ and $\hat{p}(x_k) < \hat{p}(x_{k+1})$ or $k = n$, where $\tau = \sqrt{\log\{(N^2 + N)/\alpha\}/2}$. As explained later, this implies that

$$Z_{jk} \leq Z_{jk}^{\text{iso}} \quad \text{if } \hat{p}(x_k) < \hat{p}(x_{k+1}) \text{ or } k = n. \quad (10)$$

But then it follows from Corollary 1 that $U_i^{\alpha, \text{YB}} = u_{jk}^{\text{YB}}$ is greater than or equal to

$$Z_{jk} n_{jk}^{-1} + \tau n_{jk}^{-1/2} \geq u^{\alpha/(N^2 + N)}(Z_{jk}, n_{jk}) \geq U_i^{\alpha, \text{raw}}.$$

Inequality (10) follows from a standard result about isotonic regression (see for example [Henzi et al., 2022](#), Characterization II). The index interval $\{j, \dots, k\}$ may be partitioned into index intervals $\{\ell, \dots, m\} = \{j, \dots, n\} \cap \{s : \hat{p}(x_s) = \hat{q}\}$, where \hat{q} is any value in $\{\hat{p}(x_j), \dots, \hat{p}(x_k)\}$. For such an index interval, $Z_{\ell m} \leq Z_{\ell m}^{\text{iso}}$, with equality if $\hat{q} > \hat{p}(x_j)$.

The inequality for the lower bound follows from the one for the upper bound when x_1, \dots, x_n are replaced by $1 - x_n, \dots, 1 - x_1$ and Y_1, \dots, Y_n by $1 - Y_n, \dots, 1 - Y_1$. \square

Proof of Lemma 3.2. Let $\hat{q}_1 < \dots < \hat{q}_b$ be the different elements of $\{\hat{p}(x_i) : 1 \leq i \leq n\}$, where we assume that $b \geq 2$. There exists a partition of $\{1, \dots, n\}$ into index intervals I_1, \dots, I_b such that $\hat{q}_\ell = |I_\ell|^{-1} \sum_{i \in I_\ell} Y_i$. For any integer $d \geq 1$, let M_d be the number of indices ℓ such that $|I_\ell| = d$. Since $\sum_{i \in I_\ell} Y_i \in \{0, 1, \dots, d\}$, the numbers M_d satisfy the following constraints: $M_d \in [0, d+1]$, and $\sum_{d=1}^n M_d d = n$. The question is, how large the number $b = \sum_{d=1}^n M_d$ can be under these constraints, where we drop the restriction that the M_d are integers. Suppose that $M_c < c+1$ and $M_{c'} > 0$ for integers $1 \leq c < c'$. Then we may replace $(M_c, M_{c'})$ with $(M_c + \gamma/c, M_{c'} - \gamma/c')$, where γ is the minimum of $(c+1-M_c)c$ and $M_{c'}c'$. This does not affect the constraints, but the sum $\sum_{d=1}^n M_d$ increases strictly, while $M_c = c+1$ or $M_{c'} = 0$. Eventually, we obtain an integer $d_o \geq 1$ such that $M_d = d+1$ if $1 \leq d \leq d_o$ and $M_d = 0$ for $d \geq d_o + 2$. In particular,

$$n \geq \sum_{d=1}^{d_o} (d+1)d = \frac{(d_o+2)(d_o+1)d_o}{3} > \frac{d_o^3}{3},$$

whence $d_o < (3n)^{1/3}$, while

$$b \leq \sum_{d=1}^{d_o+1} (d+1) = \frac{d_o(d_o+3)}{2} \leq Cn^{2/3},$$

where $C = 3^{2/3}(1 + 3/6^{1/3})/2 < 3$. \square

For the proof of Theorem 4.1, we need an inequality for the auxiliary function $K(\cdot, \cdot)$ in Lemma B.2 which follows from [Dümbgen \(1998, Proposition 2.1\)](#).

Lemma B.4. *For arbitrary $q \in [0, 1]$, $\xi \in (0, 1)$ and $\gamma > 0$, the inequality $K(q, \xi) \leq \gamma$ implies that*

$$|\xi - q| \leq \sqrt{2\gamma q(1-q)} + |1 - 2q|\gamma.$$

Proof of Theorem 4.1. For notational convenience, we often drop the additional subscript n , e.g. we write x_i instead of x_{ni} . For symmetry reasons, it suffices to verify the assertions about $U^{\alpha, \text{raw}}$.

In what follows, let C be a generic (large) constant which does not depend on n , but the value of which may change in each instance. It follows from Corollary 1 and Lemma B.4 that simultaneously for all $(j, k) \in \mathcal{J}$,

$$u^{\alpha/(N^2+N)}(Z_{jk}, n_{jk}) \leq \hat{p}_{jk} + C \min \left\{ \sqrt{\frac{\log(n)\hat{p}_{jk}(1-\hat{p}_{jk})}{n_{jk}}} + \frac{\log(n)}{n_{jk}}, \sqrt{\frac{\log(n)}{n_{jk}}} \right\}, \quad (11)$$

where $\hat{p}_{jk} = Z_{jk}/n_{jk}$. Moreover, one can deduce from Lemma B.2 that simultaneously for all $(j, k) \in \mathcal{J}$,

$$\hat{p}_{jk} \leq p_{jk} + C \sqrt{\frac{\log(n)}{n_{jk}}} \quad (12)$$

with asymptotic probability one, where $p_{jk} = \mathbb{E}(\hat{p}_{jk}) = n_{jk}^{-1} \sum_{i=j}^k p_i \in [p_j, p_k]$.

As to part (ii), let $B(x) = [x, x + \rho_n^{1/3}]$ for $x \in [a, b - \rho_n^{1/3}]$. For sufficiently large n , the length $\rho_n^{1/3}$ of these intervals is greater than $C_2 \rho_n$, so it follows from assumption (A) that $B(x) \cap \{x_1, \dots, x_n\} = \{x_{j(x)}, \dots, x_{k(x)}\}$ with $(j(x), k(x)) \in \mathcal{J}$ satisfying

$$n_{j(x)k(x)} = W_n\{B(x)\} \geq C_1 n \rho_n^{1/3}.$$

Consequently, $\log(n)/n_{j(x)k(x)} \leq C_1^{-1} \rho_n^{2/3}$, so we may deduce from inequalities (11), (12) and Lipschitz-continuity of p on $[a, b]$ that with asymptotic probability one, simultaneously for all $x \in [a, b - \rho_n^{1/3}]$,

$$\begin{aligned} U_n^{\alpha, \text{raw}}(x) &\leq u^{\alpha/(N^2+N)}(Z_{j(x)k(x)}, n_{j(x)k(x)}) \leq \hat{p}_{j(x)k(x)} + C \rho_n^{1/3}, \\ \hat{p}_{j(x)k(x)} &\leq p_{j(x), k(x)} + C \rho_n^{1/3}, \\ p_{j(x)k(x)} &\leq p(x) + C \rho_n^{1/3}. \end{aligned}$$

Clearly, this implies the assertion about $U^{\alpha, \text{raw}}$ in part (ii).

Part (i) can be verified similarly. With $\delta = b - b' > 0$, let $B(x) = [x, x + \delta]$ for $x \in [a, b']$. Now it follows from assumption (A) that for sufficiently large n , $B(x) \cap \{x_1, \dots, x_n\} = \{x_{j(x)}, \dots, x_{k(x)}\}$ with $(j(x), k(x)) \in \mathcal{J}$ satisfying $n_{j(x)k(x)} \geq C_1 n \delta$, uniformly for all $x \in [a, b']$. Now it follows from inequalities (11), (12) and p being constant on $[a, b]$ that with asymptotic probability one, simultaneously for all $x \in [a, b']$,

$$\begin{aligned} U_n^{\alpha, \text{raw}}(x) &\leq u^{\alpha/(N^2+N)}(Z_{j(x)k(x)}, n_{j(x)k(x)}) \leq \hat{p}_{j(x)k(x)} + C \rho_n^{1/2}, \\ \hat{p}_{j(x)k(x)} &\leq p_{j(x), k(x)} + C \rho_n^{1/2}, \\ p_{j(x)k(x)} &= p(x). \end{aligned}$$

This implies the assertion about $U^{\alpha, \text{raw}}$ in part (i).

As to part (iii), it suffices to show that $\mathbb{E}\{U_n^{\alpha, \text{raw}}(x_n)\} \leq C(x_n^\gamma + \rho_n^{1/2})$ for any sequence of numbers $x_n \in [0, 1]$ converging to 0. Let $t_n = \max(x_n, \rho_n^{1/2})$ and $B_n = [t_n, 2t_n]$. For sufficiently large n , $\text{Leb}(B_n) \geq \rho_n^{1/2} \geq C_1 \rho_n$, so $B_n \cap \{x_1, \dots, x_n\} = \{x_{j_n}, \dots, x_{k_n}\}$ with $(j_n, k_n) \in \mathcal{J}$ satisfying

$$n_{j_n, k_n} = W_n(B_n) \geq C_1 n t_n.$$

In particular, $\log(n)/n_{j_n k_n} \leq C_1^{-1} \rho_n/t_n$, and the assumption that $p(x) = \mathcal{O}(x^\gamma)$ as $x \rightarrow 0$ implies that $p_{j_n k_n} = \mathcal{O}(t_n^\gamma)$. Hence, it follows from (11) that

$$\begin{aligned}\mathbb{E}\{U_n^{\alpha, \text{raw}}(x_n)\} &\leq \mathbb{E}\{u^{\alpha/(N^2+N)}(Z_{j_n k_n}, n_{j_n k_n})\} \\ &\leq \mathbb{E}\left\{\hat{p}_{j_n k_n} + C\left(\sqrt{t_n^{-1} \rho_n \hat{p}_{j_n k_n}} + t_n^{-1} \rho_n\right)\right\} \\ &\leq p_{j_n k_n} + C\left(\sqrt{t_n^{-1} \rho_n p_{j_n k_n}} + t_n^{-1} \rho_n\right) \\ &= \mathcal{O}\left(t_n^\gamma + \rho_n^{1/2} t_n^{(\gamma-1)/2} + t_n^{-1} \rho_n\right) = \mathcal{O}_p(x_n^\gamma + \rho_n^{1/2}),\end{aligned}$$

where the last inequality follows from Jensen's inequality.

To verify part (iv), let $B_n = [x_o - C_3 \rho_n, x_o)$ for some $C_3 \geq C_2$. For sufficiently large n , $B_n \cap \{x_1, \dots, x_n\} = \{x_{j_n}, \dots, x_{k_n}\}$ with $(j_n, k_n) \in \mathcal{J}$ satisfying

$$n_{j_n k_n} \geq C_1 C_3 n \rho_n \geq C_1 C_3 \log(n) \quad \text{and} \quad p_{j_n k_n} \leq p(x_o-) < q.$$

Consequently, $\log(n)/n_{j_n k_n} \leq (C_1 C_3)^{-1}$ and thus with asymptotic probability one,

$$\begin{aligned}U_n^{\alpha, \text{raw}}(x_o - C_3 \rho_n) &\leq u^{\alpha/(N^2+N)}(Z_{j_n k_n}, n_{j_n k_n}) \leq \hat{p}_{j_n k_n} + C C_3^{-1/2}, \\ \hat{p}_{j_n k_n} &\leq p(x_o-) + C C_3^{-1/2}.\end{aligned}$$

Consequently, $U_n^{\alpha, \text{raw}}(x_o - C_3 \rho_n) < q$ with asymptotic probability one, provided that C_3 is sufficiently large. \square

References

Allison, P. J. (2014). Measures of fit for logistic regression. *Paper 1485-2014, SAS Global Forum 2014*, pages 1–12.

Bertolini, G., D'Amico, R., Nardi, D., Tinazzi, A., and Apolone, G. (2000). One model, several results: the paradox of the Hosmer-Lemeshow goodness-of-fit test for the logistic regression model. *Journal of epidemiology and biostatistics*, 5:251–253.

Clopper, C. J. and Pearson, E. S. (1934). The use of confidence or fiducial limits illustrated in the case of the binomial. *Biometrika*, 26:404–413.

Dimitriadis, T., Gneiting, T., and Jordan, A. I. (2021). Stable reliability diagrams for probabilistic classifiers. *Proceedings of the National Academy of Sciences*, 118:e2016191118.

Dümbgen, L. (1998). New goodness-of-fit tests and their application to nonparametric confidence sets. *The Annals of Statistics*, 26:288–314.

Guntuboyina, A. and Sen, B. (2018). Nonparametric shape-restricted regression. *Statistical Science*, 33(4):568–594.

Hall, P. and Horowitz, J. (2013). A simple bootstrap method for constructing nonparametric confidence bands for functions. *The Annals of Statistics*, 41:1892–1921.

Henzi, A., Moeschling, A., and Dümbgen, L. (2022+). Accelerating the pool-adjacent-violators algorithm for isotonic distributional regression. *Methodology and Computing in Applied Probability*, to appear.

Hoeffding, W. (1963). Probability inequalities for sums of bounded random variables. *Journal of the American Statistical Association*, 58:13–30.

Hosmer, D. W. and Lemeshow, S. (1980). Goodness of fit tests for the multiple logistic regression model. *Communications in Statistics - Theory and Methods*, 9:1043–1069.

Hosmer, D. W., Lemeshow, S., and Sturdivant, R. X. (2013). *Applied logistic regression*. Wiley Series in Probability and Statistics. Wiley, Hoboken, N.J, third edition.

Johnson, N. L., Kemp, A. W., and Kotz, S. (2005). *Univariate discrete distributions*. Wiley Series in Probability and Statistics. Wiley, Hoboken, NJ, third edition.

Koenker, R. and Yoon, J. (2009). Parametric links for binary choice models: A Fisherian–Bayesian colloquy. *Journal of Econometrics*, 152:120–130.

Kramer, A. A. and Zimmerman, J. E. (2007). Assessing the calibration of mortality benchmarks in critical care: The hosmer-lemeshow test revisited. *Critical care medicine*, 35:2052–2056.

Mösching, A. and Dümbgen, L. (2020). Monotone least squares and isotonic quantiles. *Electronic Journal of Statistics*, 14:24–49.

National Center for Health Statistics (2017). NCHS’ Vital Statistics Natality Birth Data. <https://data.nber.org/data/nativity.html>. Online; accessed 13 January 2021.

Nattino, G., Finazzi, S., and Bertolini, G. (2014). A new calibration test and a reappraisal of the calibration belt for the assessment of prediction models based on dichotomous outcomes. *Statistics in Medicine*, 33:2390–2407.

Nattino, G., Pennell, M. L., and Lemeshow, S. (2020a). Assessing the goodness of fit of logistic regression models in large samples: A modification of the hosmer-lemeshow test. *Biometrics*, 76:549–560.

Nattino, G., Pennell, M. L., and Lemeshow, S. (2020b). Rejoinder to “assessing the goodness of fit of logistic regression models in large samples: A modification of the hosmer-lemeshow test”. *Biometrics*, 76:575–577.

Paul, P., Pennell, M. L., and Lemeshow, S. (2013). Standardizing the power of the Hosmer–Lemeshow goodness of fit test in large data sets. *Statistics in Medicine*, 32:67–80.

Quinn, J.-A., Munoz, F. M., Gonik, B., Frau, L., Cutland, C., Mallett-Moore, T., Kissou, A., Wittke, F., Das, M., Nunes, T., Pye, S., Watson, W., Ramos, A.-M. A., Cordero, J. F., Huang, W.-T., Kochhar, S., Buttery, J., and Brighton Collaboration Preterm Birth Working Group (2016). Preterm birth: Case definition & guidelines for data collection, analysis, and presentation of immunisation safety data. *Vaccine*, 34(49):6047–6056.

R Core Team (2022). *R: A language and environment for statistical computing*. R Foundation for Statistical Computing, Vienna, Austria.

Roelofs, R., Cain, N., Shlens, J., and Mozer, M. C. (2020). Mitigating bias in calibration error estimation. *Preprint*. <https://arxiv.org/abs/2012.08668>.

Sen, B., Banerjee, M., and Woodrooffe, M. (2010). Inconsistency of bootstrap: The Grenander estimator. *The Annals of Statistics*, 38(4):1953–1977.

Shaked, M. and Shanthikumar, J. G. (2007). *Stochastic orders*. Springer Series in Statistics. Springer, New York.

Stodden, V., McNutt, M., Bailey, D. H., Deelman, E., Gil, Y., Hanson, B., Heroux, M. A., Ioannidis, J. P., and Taufer, M. (2016). Enhancing reproducibility for computational methods. *Science*, 354(6317):1240–1241.

Tutz, G. (2011). *Regression for Categorical Data*. Cambridge University Press, Cambridge.

World Health Organization (2015). *International statistical classification of diseases and related health problems*. World Health Organization. 10th revision, fifth edition. <https://apps.who.int/iris/handle/10665/246208>. Online; accessed 13 January 2021.

Wright, F. T. (1981). The asymptotic behavior of monotone regression estimates. *Annals of Statistics*, 9:443–448.

Yang, F. and Barber, R. F. (2019). Contraction and uniform convergence of isotonic regression. *Electronic Journal of Statistics*, 13:646–677.

Yu, B. and Kumbier, K. (2020). Veridical data science. *Proceedings of the National Academy of Sciences*, 117(8):3920–3929.